HEVs WITH RECONFIGURABLE ARCHITECTURE: A NOVEL DESIGN AND OPTIMAL ENERGY MANAGEMENT

Mauro G. Carignano[(a)], Norberto M. Nigro[(b)], Sergio Junco[(c)]

[(a)] EIM, Escuela de Ingeniería Mecánica, Facultad de Ciencias Exactas, Ingeniería y Agrimensura, CONICET, Universidad Nacional de Rosario, Beruti 2109, Rosario, Argentina.
[(b)] CIMEC, Centro Internacional de Métodos Computacionales en Ingeniería, INTEC-CONICET-UNL, Güemes 3450, Santa Fe, Argentina.
[(c)] LAC, Laboratorio de Automatización y Control, Facultad de Ciencias Exactas, Ingeniería y Agrimensura, Universidad Nacional de Rosario, Riobamba 250bis, Rosario, Argentina.

[(a)]mauroc@fceia.unr.edu.ar, [(b)]norberto.nigro@cimec.santafe-conicet.gov.ar, [(c)]sjunco@fceia.unr.edu.ar

ABSTRACT:
This work presents guidelines to solve the optimal energy management in hybrid electric vehicles (HEV) with reconfigurable architecture. Specifically, the vectorized implementation of Dynamic Programming (DP) is addressed. Also, a novel power-split reconfigurable architecture (PSRA) is presented and compared to the third generation of Toyota Hybrid System (THSIII). The HEVs with reconfigurable architecture use clutches to change the connection between the powertrain components. The combination of clutches provides different configurations, and as a consequence, the control input variables managed by the energy management strategy vary according to the configuration selected. This renders more complex the implementation of DP. In this work, the models and the algorithm to solve the vectorized implementation of DP in commutated-control input problems are presented. Finally, the optimal strategy is used to evaluate the performance of the novel PSRA proposed. Improvements on consumption and drivability are achieved with respect to THSIII.

Keywords: reconfigurable hybrid electric vehicle, optimal energy management, dynamic programming

1. INTRODUCTION

According to the recent life cycle assessment regarding cost and greenhouse emissions, there is not a trivial answer about what is the best platform for land transport. In (Huo et al., 2015; Onat et al., 2015; Roth, 2015) Electric, Plug-in, Hybrid and Conventional Vehicles are compared, and the results show that the lower pollutant or cheaper selection depend on the cleanness and the cost of the electricity. Due to high autonomy, low time recharge and low cost, conventional vehicles with internal combustion engine (ICE) continue being the main interest for customers and manufacturers. On the other hand, the hybrid platform improves significantly the consumption and the emissions in operations compared to conventional vehicles due both to energy recovered during the braking and to higher operating efficiency of their components. Also, the ICE-powered HEV maintain high autonomy with low time to supplying. According to these advantages, in the last 10 years the hybrid electric vehicles (HEV) have been an important and increasing segment for car manufactures.

Regarding the architecture, power-split (or combined) is the most popular and efficient architecture adopted by car manufacturers. Most of them use a planetary gear system (PGS) to divide the power between the ICE and the electric machines. One of the pioneers, Toyota Hybrid System, currently represents a highlight mark that designers try to overcome. Vinot et al. (2014) present a new virtual hybrid vehicle with an electrical variable transmission using an electric machine with a rotating external armature. The results, considering technological aspects, are comparable but not better than the first generation of THS. Zhang et al. (2013) improved the fuel consumption of the first generation of THS by adding clutches in transmission system and resizing electric machines. Along these same lines, some of the last generation split-power architecture added clutches to reconfigure the transmission system (Rahman, 2011; Si, 2011; Seo, 2012). Zhang et al. (2015a) realized an exhaustive search of the best reconfigurable architecture using exactly the same component of the Toyota Hybrid System third generation (THSIII) but adding 3 clutches. Results show improvements on the consumption and the drivability. In this work a novel power-split reconfigurable architecture (PSRA) is presented. It uses four clutches, one electric machine and one PGS. The simulation results show improvements on consumption and the drivability compared to the THSIII.

With respect to the energy management strategy (EMS) for HEV, a wide variety of methods are reported in the literature (Sciarretta et al., 2004; Guzella and Sciarretta, 2007). Particularly, for battery/ICE powered HEV, the Equivalent Consumption Minimization Strategy (ECMS) (Sciarretta et al., 2004), Load Following Strategy (Trindade et al., 2015) and offline Pontryagin's Minimum principle (PMP) (Chasse and Sciarretta,

2011) are the most widely used. All of them require an iterative procedure to find the optimal parameters that both perform the lower consumption and meet the initial/final state constraint. Furthermore, the solution provided by these methods is close to the optimal solution only in case the active constraints are not dependent on the state variables (Sciarretta et al., 2004; Guzella and Sciarretta, 2007).

Dynamic programming (DP) is widely used to solve any optimization problems and in particular to obtain the optimal solution in optimization problems associated with fuel consumption in HEV (Cariganano, 2015; Trindade et al., 2015; Vinot et al., 2014; Perez et al., 2006). The fundamentals and the formulation can be read in (Kirk, 2004), while a summarized theory with applications in HEV is described in (Guzella and Sciarretta, 2007). A disadvantage of DP is the growing of computational effort in problems with multiple-states and control inputs. A vectorized implementation reduces drastically the computational effort (Guzella and Sciarretta, 2007). Elbert and Sundström (Elbert et al., 2013; Sundström, 2010) developed DPM, a generic code to vectorized implementation of DP in Matlab. Despite its usefulness in a lot of cases of energy management in HEVs, DPM is not appropriate for reconfigurable architectures, as its code does not handle. Zhang et al. (2015a; 2015b) presents PEARS, a method to compute offline the energy management strategy in a reconfigurable architecture. Basically, PEARS consist in solving a reduced DP problem. With an error of around 3% respect to the optimal solution, the method is much faster than classic DP. Although these advantages, PEARS is a suboptimal offline strategy and its goodness is not validated in problems with active state-dependent constraints. In this work the vectorized implementation of DP to compute the optimal energy management for a reconfigurable architecture is addressed. Particularly, the pseudo-codes of the algorithms are presented and then, they are used to evaluate the performance of the PSRA proposed. The comparison of this new architecture with the THSIII shows improvement in term of consumption and drivability. To perform the simulations, a quasistatic backward model was used, which takes into account the longitudinal vehicle dynamics, battery dynamics, and efficiency maps of the engine and electric machines.

The paper is organized as follows: in section 2 the models of powertrain components, the THSIII architecture and the novel PSRA are presented; in section 3 the fundamentals of DP and the vectorized implementation are described; in section 4 the results of simulation and discussion are presented; and finally the section 5 presents conclusion and future works.

2. HEV MODELING

2.1 ICE, electric machines, battery

The ICE and the electric machines were modeled using 2D-lookup tables that express the stationary electric energy or fuel consumption. Moreover, 1D-lookup tables were used to represent the torque constraints. The following equations represent the model of a generic component "x":

$$P_x = \Phi_x(\omega_x, T_x) \tag{1}$$

$$\tau_{x,min}(\omega_x) \leq T_x \leq \tau_{x,max}(\omega_x) \tag{2}$$

$$\omega_{xmin} \leq \omega_x \leq \omega_{xmax} \tag{3}$$

where P, T and ω are consumed power, torque and speed respectively, and $\Phi \; and \; \tau$ represent maps of consumption and the curves of maximum and minimum toque respectively.

Regarding the battery, the nonlinear first order dynamic model (4)-(6) and constraints are deducted from the equivalent circuit shown in Figure 1.

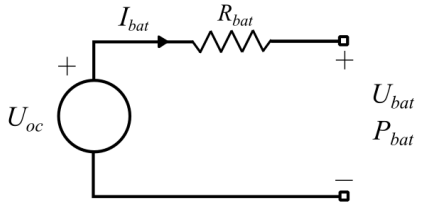

Figure 1: Battery equivalent circuit.

Using the terminal power (P_{bat}) and state of charge (SoC) as inputs, the causal model can be expressed as follows:

$$U_{oc}(SoC) = k_1 + k_2 \, SoC \tag{4}$$

$$U_{bat}(SoC, P_{bat}) = \frac{U_{oc}}{2} + \left(\frac{U_{oc}^2}{4} - P_{bat} \, R_{bat}\right)^{0.5} \tag{5}$$

$$\frac{dSoC}{dt}(SoC, P_{bat}) = -\frac{P_{bat}}{U_{bat}} C_{bat} \tag{6}$$

with the constraints:

$$U_{bat,min} \leq U_{bat} \leq U_{bat,max} \tag{7}$$

$$SoC_{min} \leq SoC \leq SoC_{max} \tag{8}$$

where $k_1, k_2, R_{bat}, C_{bat}, U_{bat,min}, U_{bat,max}, SoC_{min}$ and SoC_{max} are battery parameters, and U_{oc} and U_{bat}, are open circuit voltage and terminal voltage.

2.2 Power-split architectures

The typical three port PGS used in power-split architectures is illustrated in Figure 2. Neglecting inertia and friction efforts, the relations between torques and revolutions are described by the following equations:

$$T_s \, N_r - T_r \, N_s = 0 \tag{9}$$

$$T_c \, N_r - T_r \, (N_s + N_r) = 0 \tag{10}$$

$$\omega_s N_s + \omega_c (N_s + N_r) = \omega_r N_r \tag{11}$$

ISBN 978-88-97999-82-9; Bruzzone, Dauphin-Tanguy, Junco and Longo Eds.

where N_r and N_s are gear teeth of ring and sun respectively. According to the equations, the PGS is a particular case of a speed coupler.

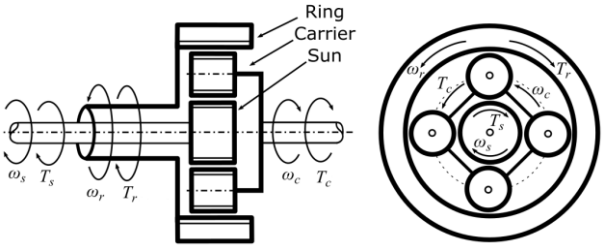

(a) Power-port variables (positive sense)

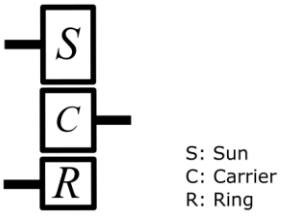

(b) Simplified representation

Figure 2: Planetary Gear System

Figure 3 shows a schematic representation of the THSIII. It is worth noticing that PGS1 works as speed coupler while the PGS2 work as a speed reducer. The electric machines and the battery are interconnected, through electronic power converters, to a direct current bus.

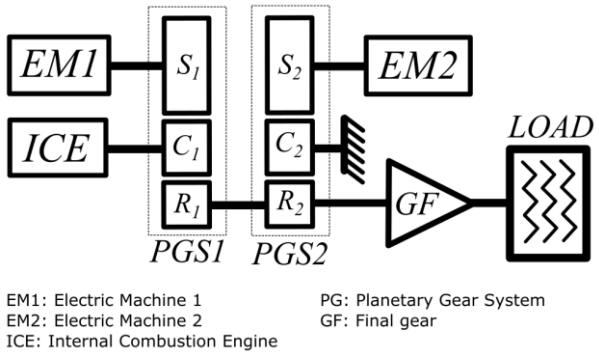

Figure 3: THSIII architecture

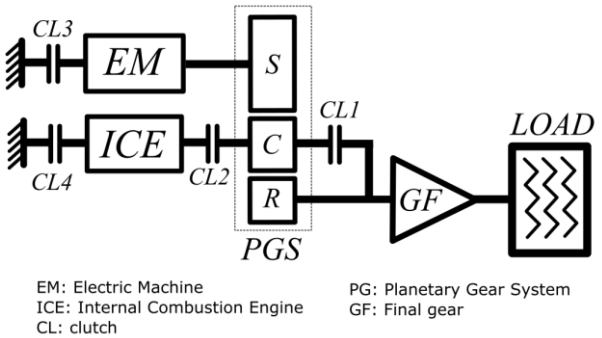

Figure 4: Novel PSRA

Figure 4 shows the novel PSRA proposed. Although 4 clutches are required, unlike THSIII, only one PGS and one electric machine are used. This PSRA has 16 different configurations associated with the states of clutches. However, most of them are unfeasible or unusable. Table 1 summarizes the useful configuration and the associated states of clutches.

Table 1: Configurations of PSRA

	Clutches			
Configuration	1	2	3	4
Electric Reduced	0	1	0	1
Electric Direct	1	0	0	0
Speed Coupling	0	1	0	0
ICE Direct	1	1	0	0
ICE Overdrive	0	1	1	0

In the *Electric Reduced* configuration, the electric machine propels the vehicle, the internal combustion engine is turned off and PGS works as a speed reducer. The *Electric Direct* is similar to the previous configuration but in this case the PGS was locked (through the clutch 1) and the connection between the electric machine and the final gear is direct. In the configuration *Split Coupling*, both the electric machine and the ICE are working and the PGS works as a speed coupler. In *ICE Direct*, the ICE propels the vehicle, the PGS works locked and the electric machine can work as motor or generator. Finally, in the *ICE Overdrive* configuration, the electric machine is locked, the ICE propels the vehicle and the PGS works as a speed multiplier.

Notice that in the first two configurations the electric machine works as generator for negative accelerations (regenerative braking). Furthermore, in *Split Coupling* configuration, depending on the vehicle speed, the electric machine works as generator (at low speed) or as motor (at high speed). These configurations, together with *ICE Direct* describes before, enable to recharge the battery, and hence operate in charge sustained condition.

2.3 Supervisory Controller

The schematic diagram shown in Figure 5 represents the quasistatic causal model of PSRA used to evaluate the HEV performance. As can be seen, in order to reduce the system order, inertias of components and low-level control loops were neglected.

The speed demand ω_d comes from the driving cycle and T_d is computed through a first order non-linear vehicle model that considers inertial forces, rolling resistance and aerodynamic drag. T_{BR} is the toque from friction brake; mf_{rate} is the fuel mass flow rate and ΔSoC_{rate} is the variation of state of charge.

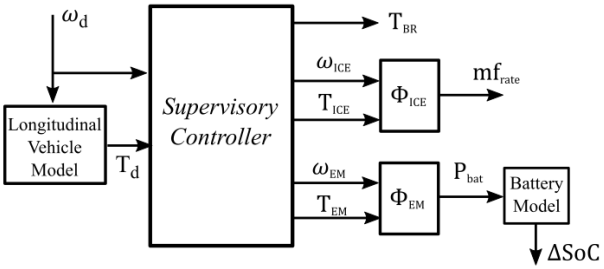

Figure 5: Schematic quasistatic causal model

The *Supervisory Controller* decides how operate the components of the propulsion system. The main purposes are to meet the driving requirement and to operate efficiently the propulsion system. Particularly in this architecture, the *Supervisory Controller* has to compute the torques and speeds of electric machine and ICE, and the torque of brakes. According to that, there are three torques $\{T_{ICE}, T_{EM}, T_{BR}\}$ and two speeds $\{\omega_{ICE}, \omega_{EM}\}$ that must be computed. Moreover, there are relations between these variables and constraints that must be met. The relations come from de PGS equations, while the constraints are associated with both speed and toque balance necessary to fulfill the driving requirements and the clutches connected to a fixed point, than imposes null speed. The set of constraint equations for each configuration are summarized in the Table 2.

Table 2: Constraint equations of PSRA

Electric Reduced	
$T_{ICE} = 0$	$\omega_{ICE} = 0$
$T_{EM}\, N_r - \frac{T_d - T_{BR}}{i_{GF}}\, N_s = 0$	$\omega_{EM}\, N_s + \omega_{ICE}\,(N_s + N_r) + -\omega_d\, i_{GF}\, N_r = 0$
Electric Direct	
$T_{ICE} = 0$	$\omega_{ICE} = 0$
$T_{EM} - \frac{T_d - T_{BR}}{i_{GF}} = 0$	$\omega_{EM} - \omega_d\, i_{GF} = 0$
Speed Coupling	
$T_{ICE}\, N_r + -\frac{T_d - T_{BR}}{i_{GF}}\,(N_s + N_r) = 0$	$\omega_{EM}\, N_s + \omega_{ICE}\,(N_s + N_r) + -\omega_d\, i_{GF}\, N_r = 0$
$T_{EM}\, N_r - \frac{T_d - T_{BR}}{i_{GF}}\, N_s = 0$	-
ICE Direct	
$T_{ICE} + T_{EM} - \frac{T_d - T_{BR}}{i_{GF}} = 0$	$\omega_{EM} - \omega_d\, i_{GF} = 0$
-	$\omega_{ICE} - \omega_d\, i_{GF} = 0$
ICE Overdrive	
$T_{ICE} - \frac{T_d - T_{BR}}{i_{GF}} = 0$	$\omega_{EM} = 0$
$T_{EM} = 0$	$\omega_{EM}\, N_s + \omega_{ICE}\,(N_s + N_r) + -\omega_d\, i_{GF}\, N_r = 0$

If the number of constraint equations is lower than the number of unknown variables, the configuration has degrees of freedom (DoF). The DoF are associated with torque or speed. Once the DoF are identified, some of the unknown variables are chosen to be considered as independent variables. These variables are called control inputs and they are computed according to the energy management strategy. Table 3 showed the DoF and the control inputs selected in each configuration.
Notice that the DoF of system and the variables used as control inputs vary depending on the configuration selected. Notice also that the choice of the variables used as control inputs is not trivial. However, in order to simplify the implementation of the energy management strategy, it is useful to select, as long as possible, the same variable for different configurations.

Table 3: DoF and control inputs of PSRA

Configuration	DoF	Control inputs
Electric Reduced	1	$\{T_{BR}\}$
Electric Direct	1	$\{T_{BR}\}$
Speed Coupling	2	$\{T_{BR},\ \omega_{ICE}\}$
ICE Direct	2	$\{T_{BR}\ , T_{ICE}\}$
ICE Overdrive	1	$\{T_{BR}\}$

On the other hand, the configuration in which operate the HEV is also decided by the supervisory controller according to the energy management strategy. This is considered as the first control input. Finally, the vector of control inputs is $\boldsymbol{u} = [u_1, u_2, u_3]$, where u_1 takes values from 1 to 5 according to the configuration selected, u_2 represents always the torque of brakes, and u_3 represents ω_{ICE}, T_{ICE} or nothing, depending on the configuration selected (see Table 3). Taking in account these statements, the set of causal equations to compute the outputs of the Supervisory Controller results as follows:

$$T_{BR} = u_2 \tag{12}$$

$$T_{ICE} = \begin{cases} 0 & if \quad u_1 = 1\ or\ 2 \\ \frac{T_d - u_2}{i_{GF}}\,\frac{N_s + N_r}{N_r} & if \quad u_1 = 3 \\ u_3 & if \quad u_1 = 4 \\ \frac{T_d - u_2}{i_{GF}} & if \quad u_1 = 5 \end{cases} \tag{13}$$

$$T_{EM} = \begin{cases} \frac{T_d - u_2}{i_{GF}}\,\frac{N_s}{N_r} & if \quad u_1 = 1\ or\ 3 \\ \frac{T_d - u_2}{i_{GF}} & if \quad u_1 = 2 \\ \frac{T_d - u_2}{i_{GF}} - u_3 & if \quad u_1 = 4 \\ 0 & if \quad u_1 = 5 \end{cases} \tag{14}$$

$$\omega_{ICE} = \begin{cases} 0 & if \quad u_1 = 1 \; or \; 2 \\ u_3 & if \quad u_1 = 3 \\ \omega_d \, i_{GF} & if \quad u_1 = 4 \\ \omega_d \, \dfrac{i_{GF} \, N_r}{(N_s + N_r)} & if \quad u_1 = 5 \end{cases} \tag{15}$$

$$\omega_{ICE} = \begin{cases} \omega_d \, \dfrac{i_{GF} \, N_r}{N_s} & if \quad u_1 = 1 \\ \omega_d \, i_{GF} & if \quad u_1 = 2 \\ \dfrac{\omega_d \, i_{GF} \, N_r - u_3 \, (N_s + N_r)}{N_s} & if \quad u_1 = 3 \\ \omega_d \, i_{GF} & if \quad u_1 = 4 \\ 0 & if \quad u_1 = 5 \end{cases} \tag{16}$$

3. DYNAMIC PROGRAMMING

For a given system, DP can be used to find the optimal control inputs that minimize a certain cost function. A detailed explanation and fundamentals of the method can be find in [Kirk, 2012] and [Guzzella, 2007]. The basic formulation of deterministic DP is described below. The vectorized algorithms to implement DP are presented in the section 3.2.

3.1 Basic Formulation

Considering the following discrete-time dynamic system:

$$\boldsymbol{x}_{k+1} = \boldsymbol{f}_{\boldsymbol{k}}(\boldsymbol{x}_k, \boldsymbol{u}_k, \boldsymbol{v}_k), \qquad k = 0,1, \dots \dots, N-1 \tag{17}$$

where $\boldsymbol{x}_k \epsilon X_k \subseteq \mathbb{R}^n$ is the vector of states; $\boldsymbol{u}_k \epsilon U_k \subseteq \mathbb{R}^m$ is the vector of control inputs; and $\boldsymbol{v}_{\boldsymbol{k}} \epsilon V_k \subseteq \mathbb{R}^v$ is the vector of disturbances (known or estimated in advance). For a given sequence of control inputs $\pi = \{\boldsymbol{u}_0, \boldsymbol{u}_1, \dots, \boldsymbol{u}_{N-1}\}$ and with initial condition $\boldsymbol{x}_0$, the following discrete-time function expresses the associated cost:

$$\boldsymbol{J}_\pi(x_0) = \boldsymbol{g}_N(x_N) + \sum_{k=0}^{N-1} \boldsymbol{g}_k \, (\boldsymbol{x}_k, \boldsymbol{u}_k, \boldsymbol{v}_k) \tag{18}$$

where $\boldsymbol{g}_k$, represent the cost to go from k to $(k+1)$, $\boldsymbol{g}_N(x_N)$ is the cost at the end, especially useful for problem with final state constrains. A sequence of control inputs denoted by π^0 is optimal if it minimizes the cost function (18), i.e.:

$$J_{\pi^0}(x_0) = \min_{\pi \epsilon \Pi} J_\pi(x_0) = J^0(x_0) \tag{19}$$

where Π represent the set of feasible sequence control inputs. Now, according to Bellman's optimality principle, if the sequence π^0 is optimal when going from $\boldsymbol{x}_0$ to $\boldsymbol{x}_N$, and $\boldsymbol{x}_i$ is a state reach in the optimal path; then, the partial sequence $\pi_i^0 = \{\boldsymbol{u}_i, \dots, \boldsymbol{u}_{N-1}\}$ taken from π^0 is the optimal sequence to go from $\boldsymbol{x}_i$ to $\boldsymbol{x}_N$, i.e.:

$$\boldsymbol{J}_{\pi_i^0}(\boldsymbol{x}_i) = \min_{\pi \epsilon \Pi} \boldsymbol{J}_\pi(\boldsymbol{x}_i) \tag{20}$$

This is the core of dynamic programming method. According to that, the optimal control inputs can be obtained solving the following equation backward in time from $k = N-1$ to 0:

$$\boldsymbol{J}_k(\boldsymbol{x}_k) = \min_{u \epsilon U_k} \{\boldsymbol{g}_k(\boldsymbol{x}_k, \boldsymbol{u}, \boldsymbol{v}_k) + \\ + \boldsymbol{J}_{k+1}(\boldsymbol{f}_k(\boldsymbol{x}_k, \boldsymbol{u}, \boldsymbol{v}_k))\} \tag{21}$$

where $\boldsymbol{J}_N(\boldsymbol{x}_N) = \boldsymbol{g}_N(\boldsymbol{x}_N)$ is computes in a first step. Notice that optimal control inputs obtained is an arrays that depend on the time and states.

3.2 Vectorized DP implementation

The process to get the optimal solution using DP can be divided in two steps. The first one computes the optimal control input matrices indexed by time and the states, and the second one performes forward simulation in time to obtain the optimal trajectory of the system from a given initial state. These processes were implemented through two subsequent algorithms: *Optimal Matrices* and *Optimal Path*.

Table 4: Variables used in the Algorithm 1

Variable	Size	Description
x	$\in \mathbb{R}^1$ $(n_x \times 1)$	State variable.
u_1	$\in \mathbb{R}^1$ (5×1)	Control input associated with the configuration selected.
u_2	$\in \mathbb{R}^1$ $(n_u \times 1)$	Control input associated with the torque of brakes.
ui	$\in \mathbb{R}^1$ $(n_u \times 1)$	Index of control inputs
Y, U_1, U_2 U_3, Ui_3	$\in \mathbb{R}^4$ $(n_x \times 5 \times n_u \times n_u)$	Rectangular grid of states, control inputs and index.
J	$\in \mathbb{R}^2$ $(n_x \times N)$	Cost matrix indexed by state and time.
SOC_{k+1}	$\in \mathbb{R}^4$ $(n_x \times 5 \times n_u \times n_u)$	Future state of charge, indexed by state and control inputs.
MF_{cons}	$\in \mathbb{R}^4$ $(n_x \times 5 \times n_u \times n_u)$	Fuel consumed in the interval $[k; k+1]$.
$MASK$	$\in \mathbb{R}^4$ $(n_x \times 5 \times n_u \times n_u)$	Ones/zeros array, according to feasible and non-feasible solution.
MG	$\in \mathbb{R}^4$ $(n_x \times 5 \times n_u \times n_u)$	Masked fuel consumption.
CTG	$\in \mathbb{R}^4$ $(n_x \times 5 \times n_u \times n_u)$	Cost to go from $(k+1)$ to the end.
C	$\in \mathbb{R}^4$ $(n_x \times 5 \times n_u \times n_u)$	Cost to go from k to the end.
C_{min}	$\in \mathbb{R}^1$ $(n_x \times 1)$	Minimum cost to go from k to the end.
iC_{min}	$\in \mathbb{R}^2$ $(n_x \times 3)$	Control input indexes of minimal cost solution.
U_1^{opt}, U_2^{opt} U_3^{opt}	$\in \mathbb{R}^2$ $(n_x \times N)$	Matrices of the optimal control inputs.

The value of the cost matrix at the end (G_N) can be used to obtain a desired final state SoC_{end}. Then, J_N is defined as null for $x = SoC_{end}$, and equal to BIG (see Algorithm 1) otherwise.

Algorithm 1: Optimal Matrices

Data:

Load parameters of ICE, electric machines and battery;

Load disturbances: ω_d, T_d ;

$BIG = 10^{10}$;

Sampling:

$x = linspace(x^{min}, x^{max}, n_x)$;

$u_1 = [1, 2, 3, 4, 5]$;

$u_2 = linspace(0, T_{BR}^{max}, n_u)$;

$u\omega_{ICE} = linspace(0, \omega_{ICE}^{max}, n_u)$;

$uT_{ICE} = linspace(0, T_{ICE}^{max}, n_u)$;

$ui = linspace(1, n_u, n_u)$;

Gridding:

$[Y, U_1, U_2, Ui_3] = ndgrid(x, u_1, u_2, ui)$;

$U_3 = u\omega_{ICE}(Ui_3) . (U_1 = 3) + uT_{ICE}(Ui_3) . (U_1 = 4)$;

Cost matrix at the end: $J(N) = G_N$;

Find Optimal Matrices:

for $k = (N-1):-1:1$ **do**

Computes Quasistatic Model in k with Y, U_1, U_2, U_3 to obtain ΔSoC and mf_{rate} ;

$SOC_{k+1} = Y + \Delta SoC(k)$;

$MF_{cons} = mf_{rate}(k) .\ \Delta t(k)$;

Computes MASK according to constraints ;

$MG = MF_{cons} . MASK + BIG . (1 - MASK)$;

1-D interpolation: $CTG = interp1(x, J(k+1), Z)$;

$C = MG + CTG$;

Find the minimum cost and indexes:

$[C_{min}, iC_{min}] = \min C\ , respec\ to\ \{U1, U2, U3\}$;

Save optimal cost: $J(k) = C_{min}$;

Save optimal control inputs:

$U_1^{opt}(k) = U_1(iC_{min})$,

$U_2^{opt}(k) = U_2(iC_{min}), U_3^{opt}(k) = U_3(iC_{min})$;

end

Once the matrix of the optimal inputs is computed, for a given initial SoC, the trajectory for the minimum fuel consumption can be obtained. Algorithms 2 shows the pseudo-code to compute the optimal path. The variables used in the code are described in Table 5.

Table 5: Variables used in the Algorithm 2

Variable	Description
u_{conf}	Configuration adopted in k.
u_{BR}	Toque of brakes in k.
u_{ICE}	Speed or Torque of ICE in k.
mf_{cons}	Accumulated fuel consumption.

Algorithm 2: Optimal Path

Data:

Load optimal input matrix: $U_1^{opt}, U_2^{opt}, U_3^{opt}$;

Load initial state: $SoC(1) = SoC_{initial}$;

Forward simulation in time:

for $k = 1:1:(N-1)$ **do**

$u_{conf} = interp1(x, U^{opt}(:, k, 1), SoC(k))$;

$u_{BR} = interp1(x, U^{opt}(:, k, 2), SoC(k))$;

$u_{ICE} = interp1(x, U^{opt}(:, k, 3), SoC(k))$;

Computes Quasistatic Model in k to obtain ΔSoC and mf_{rate} ;

$SoC(k+1) = SoC(k) + \Delta SoC(k)$;

$mf_{cons}(k+1) = mf_{cons}(k) + mf_{rate}(k)$;

end

Although the algorithm presented refer to the proposed PSRA, they can be used also for the THSIII. In this case there is only one configuration, and a possible set of control inputs are the torque of brakes, and the torque and speed of the ICE.

4. RESULTS

In this section the results of the simulations and the discussion are presented. The simulations are oriented to compare the performance of the PSRA with the THSIII in term of fuel consumption and drivability. In all cases, the optimal energy management strategy was applied, using the DP algorithm described. The fuel economy is evaluated in a combined urban-highway driving condition, and the drivability is assessed using two acceleration test.

4.1 Drivability and fuel economy

The assessment of the fuel consumption is on the basis of combined urban/highway consumption. According to the international Environmental Protection Agency (EPA), the combined fuel economy is computed as weighted average of consumptions, with 55% and 45% of urban and highway driving respectively. In this work, the *Urban Dynamometer Driving Schedule* (UDDS) was used for urban driving, and the *Highway Fuel Economy Driving Schedule* (HWFET) for highway driving. The fuel consumption is expressed in liters per $100km$ ($Lts/100$). It is worth mentioning that, in order to avoid fuel compensation due to energy consumed

from battery at the end of the cycle, the charge sustained condition (i.e. $SOC(1) = SOC(end)$) was imposed for both architectures.
On the other hand, the drivability is assessed on the basis of two widely spread acceleration tests. The first one computes the time required to go from 0 to 100 $km\ h^{-1}$; and the second one the time required to go 1000 m starting from idle.

4.2 Toyota Prius

The first vehicle evaluated was the well-known Toyota Prius, which uses the THSIII architecture. The parameters of the vehicles and characteristic of components are summarized in Table 6 (Burress et al., 2011).

Table 6: Toyota Prius third generation

Chassis	Total mass	1459 Kg
	Frontal area	2.304 m^2
	Drag coefficient	0.25
	Rolling resistance	0.015 $7\,.10^{-6} m^2 s^{-2}$
Engine	Max. Power	73 kW to 5200 RPM
	Max. Torque	142 Nm to 3800 RPM
Electric Machine 1	Max. Power	42 kW
	Max. Speed	1000 RPM
Electric Machine 2	Max. Power	60 kW
	Max. Speed	1300 RPM
Battery	NiMH Cells	168
	Max Power	22 kW $to\ SoC = 0.7$
	Capacity	23400 As
	Resistance	0.336 Ω
Planetary Gear System 1	Sun teeth, N_{s1}	30
	Ring teeth, N_{r1}	78
	Efficiency	0.95
Planetary Gear System 2	Sun teeth, N_{s2}	22
	Ring teeth, N_{r2}	58
	Efficiency	0.95
Differential	Final Gear, i_{GF}	3.26

Table 7: Performance of Toyota Prius

Combined consumption	4.498 $Lts/100$
Test 0 a 100 $Km.h^{-1}$	12.0 s
Test 0 a 1000 m	32.8 s

The results of simulation to the fuel economy and drivability are presented in Table 7.

4.3 Optimized THSIII and PSRA

The proposed RPSA was assembled with the components of the Toyota Prius. However, as it was shown previously, the novel PSRA required only one electric machine and only one PGS. Specifically, the PGS 2 and the Electric Machine 1 were used. Also, in PSRA, the size of battery was increases from 168 to 366 cell, which provides a maximum discharge power of 44kW to $SoC = 0.7$. On the other hand, the teeth gear of the PGS and the final gear were tuned.
In order to perform a fair comparison between the PSRA and THSIII architecture, both were optimized through a parametric sweep, varying the final gear and PGS. Specifically, the final gear ratio and the teeth of ring of the PGS are varying as shown in Table 8.

Table 8: Parametric sweep

	THSIII		
	Min	Max	$Step$
i_{GF}	3	3.9	0.15
N_{r1}	70	100	10
N_{r2}	50	90	10

	PSRA		
	Min	Max	$Step$
i_{GF}	3	3.9	0.15
N_r	70	100	10

It was observed that fuel economy as well as drivability are affected by these parameters. The final design adopted in both architectures was that achieved the minimum combined consumption, maintaining (or improving) the drivability of the Toyota Prius. According to that, the optimal fuel economy designs result as shown in Table 9. Finally, the fuel economy and drivability obtained with PSRA, THSIII and Toyota Prius are shown in Table 10.

Table 9: Optimal fuel economy designs

	THSIII
i_{GF}	3.45
N_{r1}	80
N_{r2}	60

	PSRA
i_{GF}	3.6
N_r	60

Table 10: Optimal fuel economy designs

	Toyota Prius	Optimized THSIII	Novel PSRA
Combined consumption [$Lts/100$]	4.498	4.491	4.385
Test 0 a 100 $Km.h^{-1}$ [s]	12.0	11.7	10.9
Test 0 a 1000 m [s]	32.8	32.8	30.8

As can be seen, the improvements on consumption and drivability of the optimized-THSIII respect to Toyota Prius are minor. This is to be expected since the optimum final design resulting is close to the standard Toyota Prius. On the other hand, the novel PSRA proposed shows improvement on both, drivability and consumption. Specifically, 2.5% on consumption and around 10% on acceleration tests.

5. CONCLUSION

The work presents models and guidelines to solve the problem of optimal energy management using DP in a HEV with reconfigurable architecture. The pseudo-codes of the algorithms of a vectorized implementation of DP were presented. Despite these algorithms are referred to the reconfigurable architecture proposed, it is

worth mentioning that they are general enough to cover a wide range of problems concerning the vectorized implementation of DP.

Regarding the novel architecture proposed, compared to the THSIII, it uses only one electric machine and only one PGS. However, four clutches were used and a larger battery was required. In view of the results of simulations, the architecture proposed is a potential solution as architecture of HEV, since it improves both fuel economy and drivability compared to the THSIII.

ACKNOWLEDGMENTS

The authors wish to thank SeCyT-UNR (the Secretary for Science and Technology of the National University of Rosario) for its financial support through project PID-UNR 1ING387, ANPCyT (PICT 2012 Nr. 2471), and CONICET, the Argentine National Council for Scientific and Technological Research.

REFERENCES

Burress, T. A., Campbell, S. L., Coomer, C., Ayers, C. W., Wereszczak, A. A., Cunningham, J. P., ... & Lin, H. T., 2011. Evaluation of the 2010 Toyota Prius hybrid synergy drive system. Oak Ridge National Laboratory; Power Electronics and Electric Machinery Research Facility.

Carignano, M. G., Nigro, N. M. and Junco S., 2015. Hybridization effect on fuel consumption and optimal sizing of components for hybrid electric vehicles. Proceedings of Integrated Modeling and Analysis in Applied Control and Automation, 48-54.

Chasse, A., & Sciarretta, A., 2011. Supervisory control of hybrid powertrains: an experimental benchmark of offline optimization and online energy management. Control Engineering Practice, 19(11), 1253-1265.

Elbert, P., Ebbesen, S., and Guzzella, L., 2013. Implementation of Dynamic Programming for-Dimensional Optimal Control Problems With Final State Constraints. Control Systems Technology, IEEE Transactions on, 21(3), 924-931.

Guzzella, L., and Sciarretta, A., 2007. Vehicle propulsion systems (Vol. 1). Springer-Verlag Berlin Heidelberg.

Huo, H., Cai, H., Zhang, Q., Liu, F., & He, K., 2015. Life-cycle assessment of greenhouse gas and air emissions of electric vehicles: A comparison between China and the US. Atmospheric Environment, 108, 107-116.

Kirk, D. E., 2012. Optimal control theory: an introduction. Courier Corporation.

Onat, N. C., Kucukvar, M., & Tatari, O., 2015. Conventional, hybrid, plug-in hybrid or electric vehicles? State-based comparative carbon and energy footprint analysis in the United States. Applied Energy, 150, 36-49.

Pérez, L. V., Bossio, G. R., Moitre, D., & García, G. O., 2006. Optimization of power management in an hybrid electric vehicle using dynamic programming. Mathematics and Computers in Simulation, 73(1), 244-254.

Rahman, K., Anwar, M., Schulz, S., Kaiser, E., Turnbull, P., Gleason, S., & Grimmer, M., 2011. The voltec 4ET50 electric drive system. SAE International Journal of Engines, 4(1), 323-337.

Roth, M., 2015. Lifetime Costs, Life Cycle Emissions, and Consumer Choice for Conventional, Hybrid, and Electric Vehicles. In Transportation Research Board 94th Annual Meeting (No. 15-5314).

Sciarretta, A., & Guzzella, L., 2007. Control of hybrid electric vehicles. Control systems, IEEE, 27(2), 60-70.

Sciarretta, A., Back, M., & Guzzella, L., 2004. Optimal control of parallel hybrid electric vehicles. Control Systems Technology, IEEE Transactions on, 12(3), 352-363.

Seo, K., and Yang, H., 2012, Powertrain for Hybrid Vehicle, U.S. Patent No. 8,147,367.

Si, B., 2011. Reconfiguration Hybrid Powertrain. U.S. Patent No. 0,319,211.

Sundström, O., Ambühl, D., & Guzzella, L., 2010. On implementation of dynamic programming for optimal control problems with final state constraints. Oil & Gas Science and Technology–Revue de l'Institut Français du Pétrole, 65(1), 91-102.

Trindade, I. M. and Fleury A., 2015. Modelling, control and application of dynamic programming to a series-parallel hybrid electric vehicle. Proceedings Integrated Modeling and Analysis in Applied Control and Automation, 71-78.

Vinot, E., Trigui, R., Cheng, Y., Espanet, C., Bouscayrol, A., & Reinbold, V., 2014. Improvement of an EVT-based HEV using dynamic programming. Vehicular Technology, IEEE Transactions on, 63(1), 40-50.

Zhang, X., Peng, H., & Sun, J.,2013. A near-optimal power management strategy for rapid component sizing of power split hybrid vehicles with multiple operating modes. In American Control Conference, 2013, pp. 5972-5977. IEEE.

Zhang, X., Li, S. E., Peng, H., & Sun, J.,2015. Efficient Exhaustive Search of Power-Split Hybrid Powertrains With Multiple Planetary Gears and Clutches. Journal of Dynamic Systems, Measurement, and Control, 137(12), 121006.

Zhang, X., Peng, H., & Sun, J., 2015. A near-optimal power management strategy for rapid component sizing of multimode power split hybrid vehicles. Control Systems Technology, IEEE Transactions on, 23(2), 609-618.

AUTHOR BIOGRAPHY

Mauro Carignano received the Mechanical Engineering degree from Facultad de Ciencias Exactas Ingeniería y Agrimensura de la

Universidad Nacional de Rosario, Rosario, Argentina, in 2011. He is currently working toward the Ph.D. degree. His research interests include optimal sizing of components and strategies of high level supervisory control for hybrid electric vehicles.

Norberto M. Nigro received the Mechanical Engineer degree at Universidad Tecnologica Nacional de Buenos Aires in 1985, and his doctor degree at Engineering Sciences in Universidad Nacional de Cordoba in 1993, working under the direction of Sergio Idelsohn in topics related to FEM solutions to CFD problems, especially stabilization. In 1994-1995 he realized a postdoc stage in Minnesota Supercomputer Institute under the advisory of Tayfun Tezduyar. Since 1996 he is Researcher at CONICET (National Council of Science and Technology in Argentina). At present he is Principal Researcher of CONICET and Associate Professor of Universidad Nacional del Litoral at Santa Fe, Argentina in topics related with multiphase reactive flow problems by CFD with applications in energy management, in particular internal combustion engines, oil & gas and nuclear industries. Also his interest lies on external aerodynamics of vehicles.

Sergio Junco received the Electrical Engineer degree from the *Universidad Nacional de Rosario* (UNR) in 1976. In 1982, after 3 years in the steel industry and a 2-year academic stage at the University of Hannover, Germany, he joined the academic staff of UNR, where he currently is a Full-time Professor of System Dynamics and Control and Head of the Automation and Control Systems Laboratory. His current research interests are in modeling, simulation, control and diagnosis of dynamic systems, with applications in the fields of motion control systems with electrical drives, power electronics, mechatronics, vehicle dynamics and smart grids. He has developed, and currently teaches, several courses at both undergraduate and graduate level on System Dynamics, Bond Graph Modeling and Simulation, Advanced Nonlinear Dynamics and Control of Electrical Drives, as well as Linear and Nonlinear Control with Geometric Tools.